



Electrowinning of tellurium from alkaline leach liquor of cemented Te

Y.-C. HA¹, H.-J. SOHN¹, G.-J. JEONG², C.K. LEE³ and K.-I. RHEE³

¹School of Materials Science and Engineering, Seoul National University, Seoul, 151-742, Korea;

²Department of Mineral and Petroleum Engineering, Seoul National University, Seoul, 151-742, Korea;

³Minerals & Materials Processing Division, Korea Institute of Geology, Mining & Materials, 30 Kajung Dong, Yusong-Ku, Taejon, 305-350, Korea

Received 5 February 1999; accepted in revised form 20 July 1999

Key words: alkaline leach liquor, cemented Te, electrodeposition, electrowinning, tellurium

Abstract

The electrochemical behaviour of tellurium in 2.5 M NaOH solution was studied for the recovery of tellurium from alkaline leach liquor of cemented Te using steady state polarization and cyclic voltammetry. The deposition characteristics and the potential range for a stable deposit of tellurium were also investigated. The morphology of deposited Te in alkaline solution showed a very porous nature and needlelike radial growth. The potential range for stable electrodeposition was between -0.8 V and -0.95 V (vs Hg/HgO electrode), but electrowinning could be carried out at more negative potentials due to the disproportionation reaction of Te_2^{2-} . Laboratory-scale electrowinning experiments were performed under different operating voltages, temperatures and initial Te concentrations. The current efficiency was about 85–90% for 50% recovery and about 50–60% for 90% recovery. The purity of electrodeposited Te was higher than 99.95%.

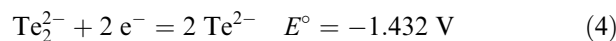
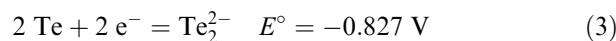
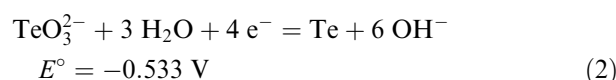
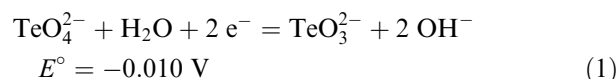
1. Introduction

Various processes for the recovery of tellurium from copper anode slimes were reviewed by Hoffmann [1]. However, each process has its own drawbacks, for example, the high oxygen and reagent consumption or the difficulties in the separation of Se. The chlorination process recommended by Hoffmann [1] has many advantages in rapid reaction, easy control and fast turnover of the precious metals in the slimes, but some problems associated with using corrosive media exist.

Recently, a series of hydrometallurgical processes involving alkaline leaching, purification and electrowinning was tested to produce pure Te metal from cemented Te [2]. In these studies Te was readily extracted up to 99% by NaOH leaching. Most of the impurities such as Cu, Pb and Fe, Bi remained as a residue, and further amounts of impurities in the solution were removed by precipitation with Na_2S . Te metal was recovered up to 95% from the purified solution by electrowinning. The level of impurities in the solution such as Se and As changed little during electrowinning.

It is necessary to understand the electrochemical behaviours of tellurium in alkaline leach liquor for the optimization of the electrowinning process. Studies on the electrochemistry of tellurium and its ionic species in alkaline solution have been sparse, except for the early polarographic investigations [3–5], comparison of the use of polarographic, coulometric and stationary elec-

trode methods [6] and a RRDE study on telluride ions [7]. The results were consistent with thermodynamic analysis [8] and the following reactions were expected as the potential was lowered at pH above 11:



The equilibrium potential for each reaction was calculated assuming a pH of 14 and an ionic species concentrations of 10^{-3} M with an activity coefficient of unity, respectively, and the potential value is given relative to the Hg/HgO electrode (0.075 V vs SHE).

In the present study, the electrochemical behaviour of tellurite, especially Equations 2 and 3, were investigated to obtain the characteristics of the electrodeposition of tellurium in alkaline solution. To optimize the electrowinning process, the potential range for a stable deposit of tellurium was also studied and laboratory-scale electrowinning experiments under different conditions were carried out.

2. Experimental details

Solutions were prepared from reagent grade chemicals (Aldrich) dissolved in 2.5 M NaOH solution (10 mM TeO_3^{2-}). The NaOH concentration was the same as that on the leaching process. The leach liquor used for electrowinning was prepared according to the previous study [2], and the different initial Te concentrations were obtained by leaching the cemented Te with the different pulp densities. Te was extracted up to 99% within 20 min in the case of 100–200 g dm^{-3} pulp density. The impurities were precipitated with the addition of Na_2S (4 g dm^{-3}) at 80 °C for 2 h and the concentrations of As and Se after purification were about 1.5 g dm^{-3} and 300 ppm, respectively, and those of other impurities such as Cu, Pb and Fe were below the order of ppm.

A Hg/HgO (in 2.5 M NaOH solution) electrode was used as reference electrode (0.075 V vs SHE) and its potential was calibrated using a saturated calomel electrode (SCE). All potentials in this work are quoted with respect to the Hg/HgO reference electrode. A Pt or Te disc electrode (dia. 1 cm) was used as working electrode. Pt (dia. 0.5 mm) and Te (dia. 1.0 mm) electrodes were also used for cyclic voltammetry experiments. A Pt plate served as counter electrode. Te disc electrodes were fabricated by grinding Te powder (>99.95%, –200 mesh size), pressing under 1500 kg cm^{-2} followed by sintering at 300 °C for an hour under Ar atmosphere. The density of a Te disc was about 85% of the theoretical value for crystalline tellurium. All working electrodes were finally polished with 0.05 μm alumina (Buehler) before each experiment.

For practical application, a stainless steel (SS304) rotating disc electrode was also used as a working electrode for polarization experiments and SS plates were used as both anode and cathode for laboratory-scale electrowinning experiments.

All experiments were performed with an EG&G PARC model 273A system. The morphology of the deposited tellurium was analyzed by SEM (Philips XL20), the structure by XRD (Mac Science MXP18A-HF) and the purity by ICP-AES (Shimadzu ICPS-1000IV).

3. Results and discussion

3.1. Electrochemical behaviour of tellurium

3.1.1. Cathodic polarization

Based on the Pourbaix diagram [8], tellurite ion (TeO_3^{2-}) undergoes stepwise reduction to Te^0 , Te_2^{2-} and finally Te^{2-} , as mentioned previously. Figure 1 shows the cathodic polarization curve of TeO_3^{2-} (10 mM) in 2.5 M NaOH solution on a Pt rotating disc electrode. The sweep was initiated from the rest potential with a scan rate of 0.166 mV s^{-1} and a rotation speed of 300 rpm. The first current plateau is the limiting current for the reduction of dissolved oxygen. At potentials

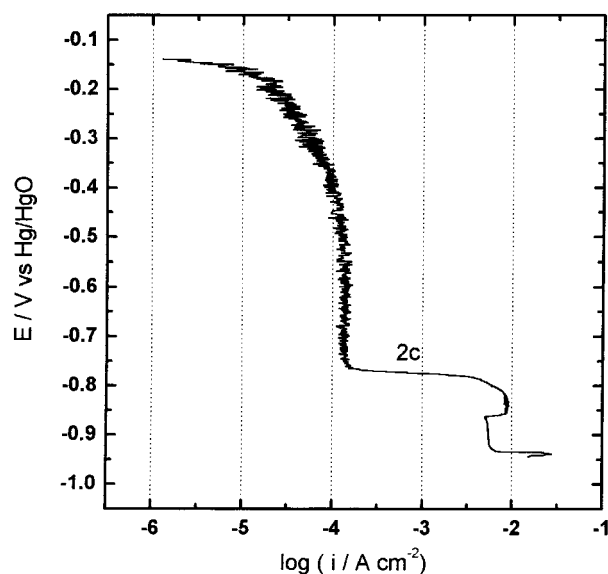


Fig. 1. Cathodic polarization curve (scan rate 0.166 mV s^{-1}) at a Pt RDE in 2.5 M NaOH solution containing 10 mM TeO_3^{2-} (rotation speed 300 rpm).

about -0.76 V, the reduction current of TeO_3^{2-} to Te^0 (2c) increased sharply. After this sharp increase the current profile at more negative potentials became complicated due to a possible reduction reaction of Te^0 to Te_2^{2-} and hydrogen evolution, which caused breakdown of deposited Te.

To identify the reduction of Te^0 to Te_2^{2-} , a Te rotating disc electrode was polarized from the rest potential to -0.9 V (Figure 2). The first shoulder (2c) is the reduction of tellurite ion within the pores of the porous Te electrode produced during polarization. Unlike Pt the overpotential to reduce tellurite was relatively small. After passing the region of the limiting current for tellurite ions, the second reaction (3c) can be

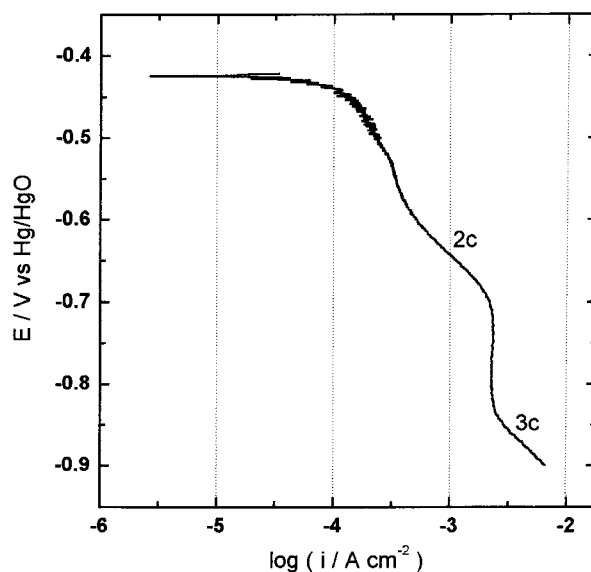


Fig. 2. Cathodic polarization curve (scan rate 0.166 mV s^{-1}) at a Te RDE in 2.5 M NaOH solution (rotation speed 300 rpm).

assigned to the reduction of tellurium to ditelluride ion due to the change of color of the solution from colorless to purple.

The above argument for the shoulder 2c was confirmed by linear sweep voltammetry. Figure 3 shows the reduction behaviour of a Te electrode (dia. 1 mm) with different polarization times (τ) at -0.4 V. With increasing τ , the peak 2c increased due to the increase in concentration of tellurite ion produced during polarization, but the peak 3c was independent of τ . The reduction potentials of 2c and 3c were virtually in accordance with the calculated values (assuming pH = 14, -0.533 V for Reaction 2 with $[\text{TeO}_3^{2-}] = 10^{-3}$ and -0.738 V for Reaction 3 with $[\text{Te}_2^{2-}] = 10^{-6}$).

3.1.2. Cyclic voltammetry

CV experiments were carried out to investigate the electrochemical behaviour of tellurite. Figure 4 illustrates the CV data at a Pt disc electrode between -0.85 V and 0.30 V. The scan was initiated cathodically from the rest potential and the disc was rotated at 300 rpm. The cathodic part of the curve shows a crossover between the cathodic and the anodic scans, which indicates typical phase formation and growth. This behaviour can be found in other studies on the electrodeposition of metals on different substrates and explained as a nucleation and growth process [9–11]. A large nucleation overpotential is necessary for the reduction of tellurite on Pt during the cathodic scan and the current increases sharply after the formation of the nuclei. During the anodic scan the overpotential for the reduction of tellurite on the nucleated Te is relatively small, which shows the crossover of the cathodic current.

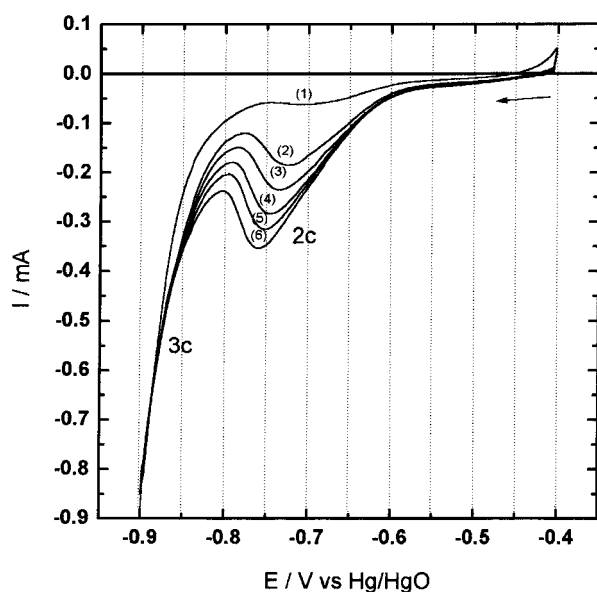


Fig. 3. Linear sweep voltammograms (scan rate 0.1 V s^{-1}) at a Te electrode (dia. 1 mm) in 2.5 M NaOH solution. Polarization (τ) at -0.4 V: (1) 0, (2) 5, (3) 10, (4) 20, (5) 30 and (6) 60 s.

On the one hand, the anodic current (peak 2a) increased with cycling and the ratio of the cathodic charge to the anodic charge approached unity after the 5th cycle. On the other hand, when the rotation was stopped, the peak 2a was virtually unchanged as shown in Figure 5. This behaviour can be explained by the deposition characteristics and the low electrical conductivity of tellurium. Without convection, the growth of nuclei deposited on the metal surface proceeded radially, which would deplete the tellurite ion near the surface,

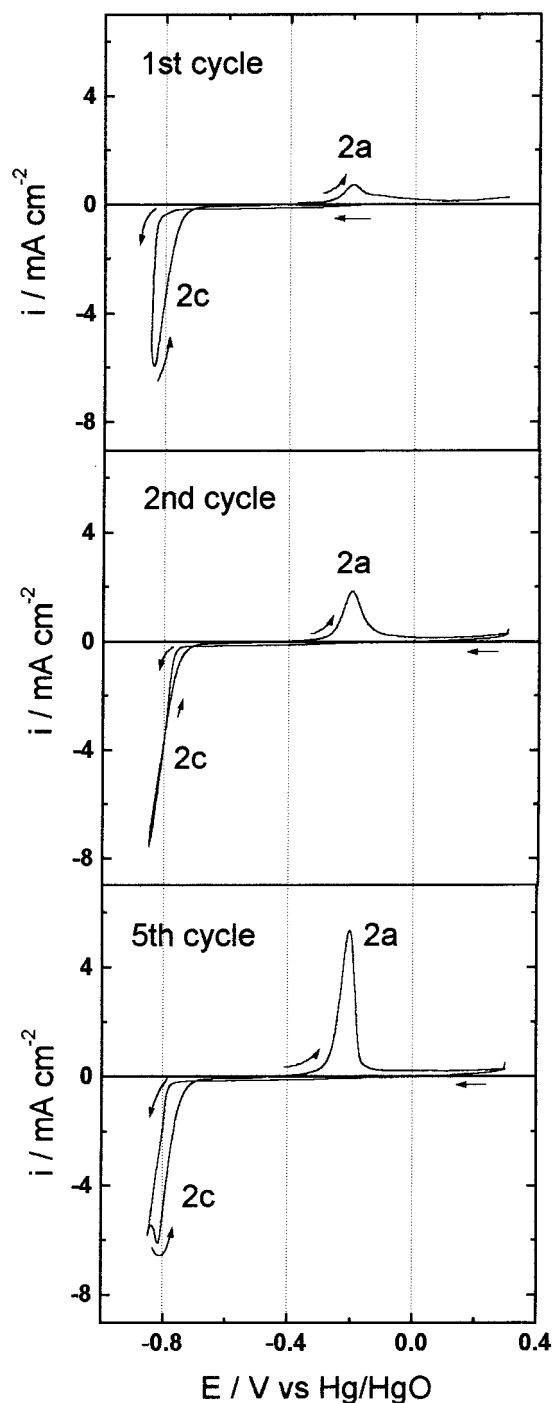


Fig. 4. Cyclic voltammograms (scan rate 0.01 V s^{-1}) at a Pt disc electrode in 2.5 M NaOH containing 10 mM TeO_3^{2-} (rotating speed 300 rpm).

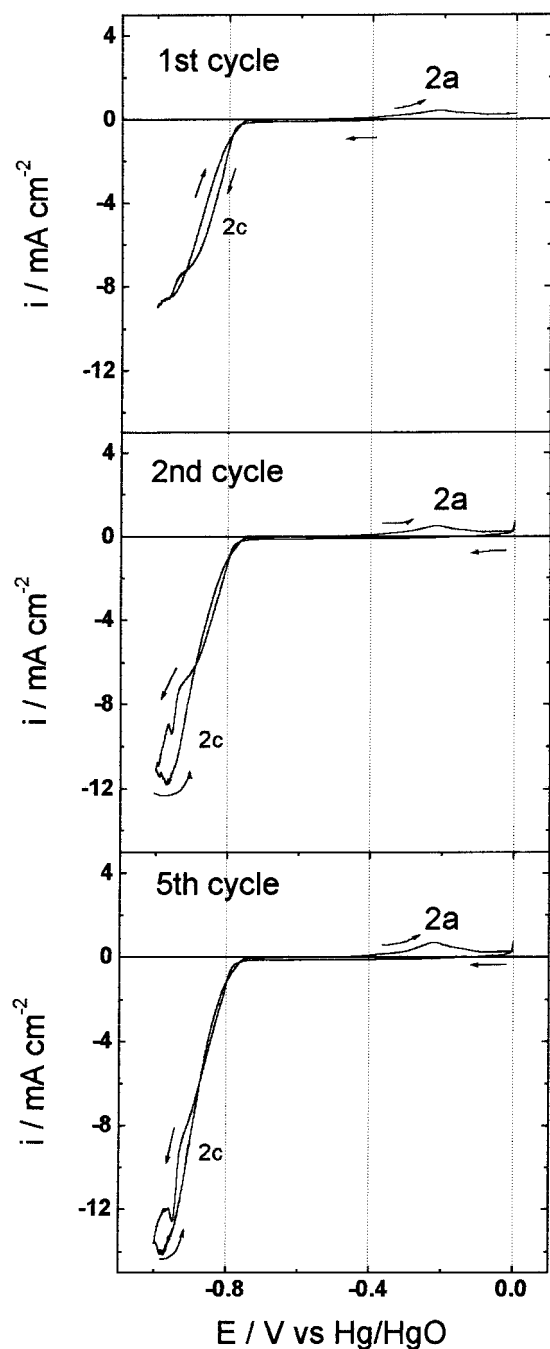


Fig. 5. Cyclic voltammograms (scan rate 0.01 V s^{-1}) at a stationary Pt disc electrode in 2.5 M NaOH containing 10 mM TeO_3^{2-} .

and the deposit would grow predominantly from protruding tips into the bulk solution. During the anodic scan, tellurium began to dissolve from the root of the protrusion because of the low electrical conductivity and 'dead tellurium' was produced near the metal surface. These protrusions and 'dead tellurium' were easily observed by sight. However, at a rotated disc the density of nuclei is higher and the lateral growth between the nuclei makes a compact deposit with good electrical conductivity.

Figure 6 shows the cyclic voltammograms of a Pt electrode (dia. 0.5 mm) in tellurite solution at different scan rates (v). On the one hand, the cathodic peak $2c$ is

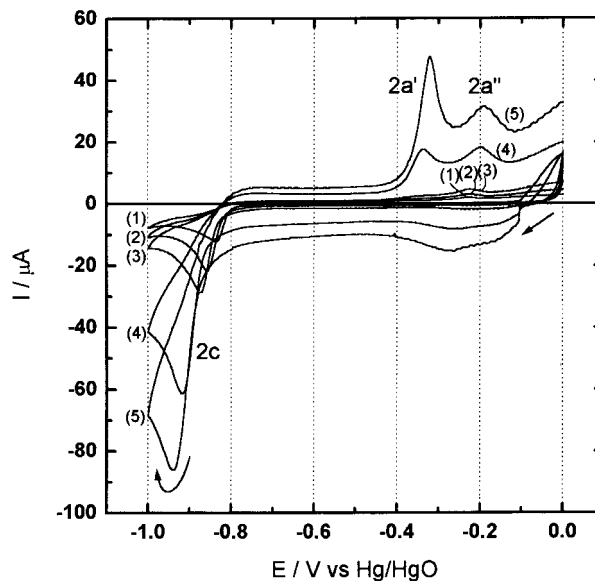
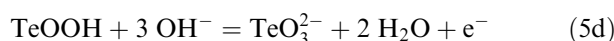
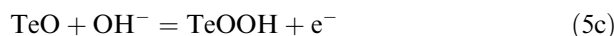
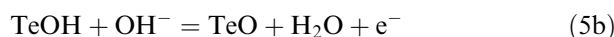


Fig. 6. Cyclic voltammogram at a Pt electrode (dia. 0.5 mm) in 2.5 M NaOH containing 10 mM TeO_3^{2-} . Scan rate, v : (1) 0.02 , (2) 0.05 , (3) 0.1 , (4) 0.5 and (5) 1.0 V s^{-1} .

simply a reduction of tellurite ion to tellurium as mentioned. The peak current I_p is found to be linear with $v^{1/2}$, indicating diffusion control. On the other hand, the anodic peaks $2a'$ and $2a''$ are separated with increasing scan rate. These show the intermediate steps of oxidation of tellurium. According to Zhdanov [12], the anodic oxidation of tellurium in alkaline solution takes place as follows:



In highly alkaline solution, step 5d is rate-determining [12]. In this respect, the anodic peak $2a''$ may be assigned to step 5d and the peak $2a'$, which exhibited a shoulder at low scan rate, may be assigned to the intermediate steps prior to the rate-determining step.

The oxidation reaction of ditelluride ion to tellurium was investigated using the Te disc electrode in pure 2.5 M NaOH solution. The cyclic voltammogram with $v = 0.01 \text{ V s}^{-1}$ is shown in Figure 7. The peak $3a$ increases with cycle number and represents the oxidation of ditelluride ion.

From the above polarization and cyclic voltammetry experiments, the potential range for the electrodeposition of tellurium on metals such as Pt was found to be very narrow (within 150 mV). For electrowinning of Te, however, more negative potentials can be allowed if a stable deposit is not necessary. In this case the deposited Te can be detached from the cathode surface by hydrogen evolution and a filtration process to recover

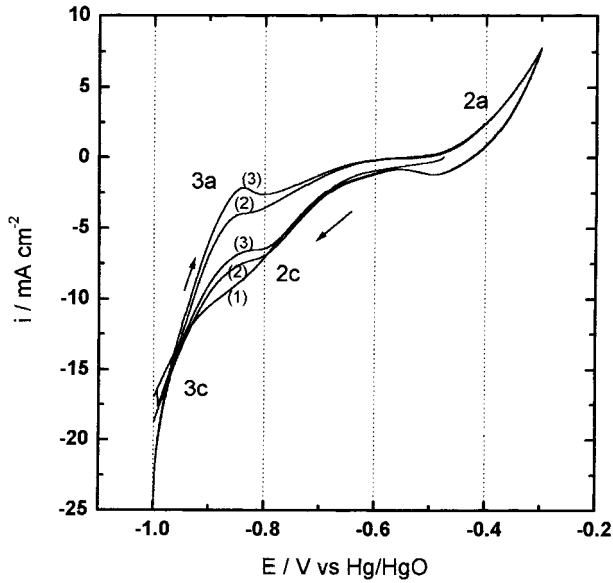


Fig. 7. Cyclic voltammogram (scan rate 0.01 V s^{-1}) at a Te disc electrode (dia. 1 mm) in 2.5 M NaOH solution. Cycles: (1) 1st, (2) 2nd and (3) 3rd.

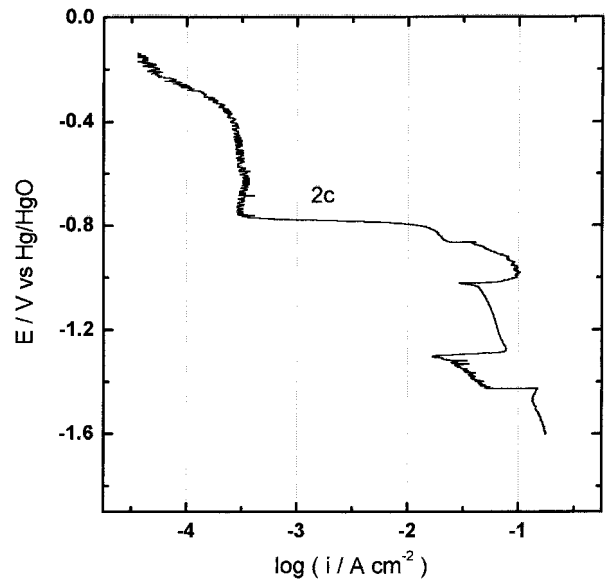
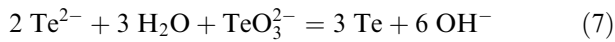


Fig. 8. Cathodic polarization curve (scan rate 0.5 mV s^{-1}) at an SS RDE in 2.5 M NaOH solution containing 10 mM TeO_3^{2-} (rotation speed 300 rpm).

the tellurium is necessary. Moreover the Te dissolution to ditelluride ion is not important since the following reactions occur [7, 13].



The telluride ion produced by disproportionation, Reaction 6, reacts with incoming tellurite ion, which precipitates as colloidal Te.

3.2. Electrowinning of tellurium from alkaline leach liquor

3.2.1. Electrodeposition

From a practical point of view, the deposition characteristics were studied on SS electrodes. Figure 8 shows the cathodic polarization curve for an SS rotating disc electrode with 2.5 M NaOH containing 10 mM TeO_3^{2-} . Similar to the Pt electrode, as shown in Figure 1, a sharp current increase near the potential about -0.76 V was observed, indicating the necessary nucleation overpotential on SS.

Figure 9(a) shows the SEM image of the above electrode focused near the center of the disc, which was polarized up to a potential of -0.85 V . Tellurium was deposited along the streamlines of the rotating disc electrode. Similar deposition characteristics were reported in studies of zinc deposition [14]. In this study the striations following the streamline was explained by the negative values of $(\partial i / \partial C)_\eta$, that is, the dependence of current density on surface concentration at constant

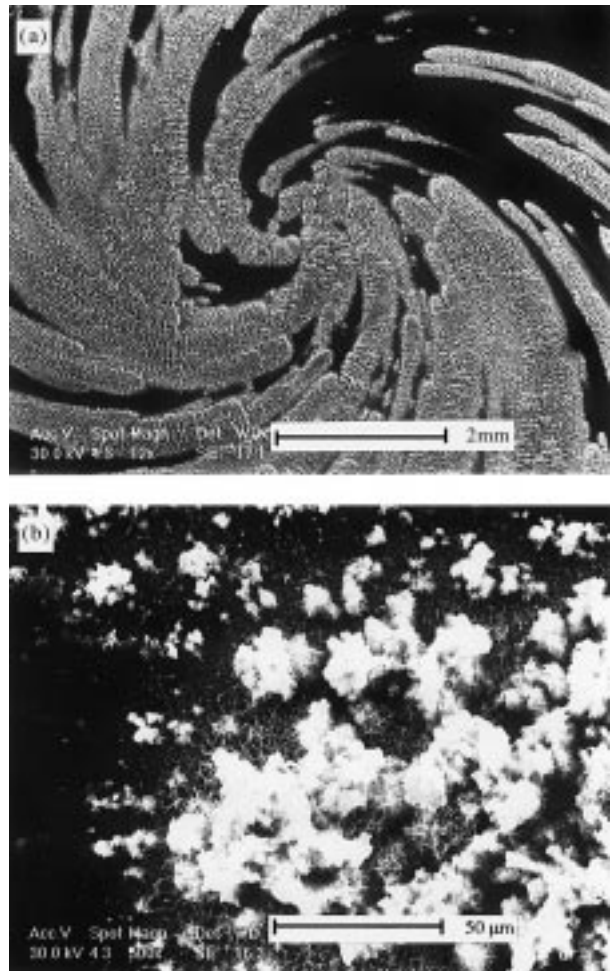


Fig. 9. Morphology of the tellurium deposit on an SS RDE. The potential was scanned up to -0.85 V .

overpotential, which usually results in a negative or small polarization resistance. The polarization resistance for deposition of tellurium was also small, as shown in Figure 8. Figure 9(b) shows the head of the deposit, where some grown particles and a complex network of needlelike deposits between the particles are observed.

For the potentiostatic experiments a SS plate was used as a cathode (area 4 cm^2), and the electrolyte was an alkaline leach liquor of cemented Te. Figure 10 illustrates the current time behaviour for a potentiostatic experiment with an applied potential of -0.8 V . The current increased with time due to the increase in surface area of tellurium deposited and then became steady. After about 5 h the limiting current gradually decreased due to the decrease in bulk concentration. Figure 11 shows the SEM images of the deposit. Growth occurred predominantly in the normal direction followed by needlelike radial growth within the pores of the deposit. At more positive potentials than -0.8 V , tellurium could not be deposited over the entire plate but deposited locally, and growth in the normal direction was preferred to that in the lateral direction. At more negative potentials than about -0.95 V , the deposit was structurally unstable due to rapid growth in the normal direction and dissolution to Te_2^{2-} , so that it was broken away by the flow of solution or by hydrogen evolution at the cathode surface.

Figure 12 shows the XRD pattern of the electrodeposited tellurium at an applied potential of -0.8 V and all peaks in the figure represent the hexagonal tellurium structure.

Among the impurities in the leach liquor, Cu has a relatively positive reduction potential in highly alkaline solution and readily deposits with tellurium during electrowinning. But Na_2S purification minimizes the Cu content below the order of ppm [2]. The concentration

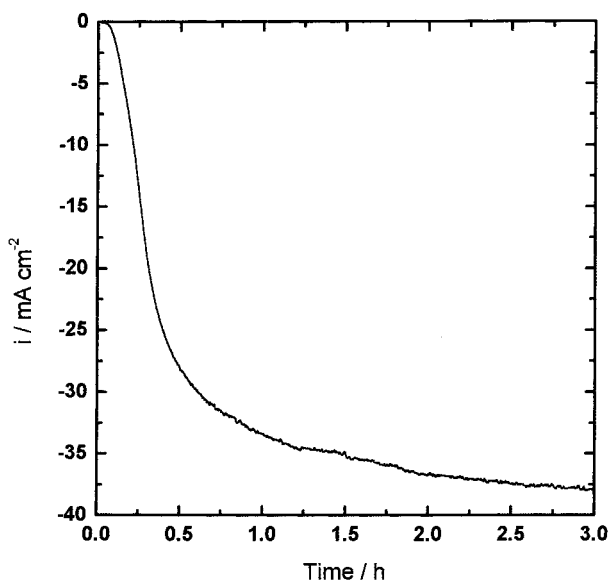


Fig. 10. Current profile with applied potential of -0.8 V at an SS plate (area 4 cm^2) in the alkaline leach liquor of cemented Te.

of Pb, which had been studied as major impurities with Se in alkaline leach liquor [13], was also below the order of ppm. Other impurities than Se have much more negative reduction potentials than that of Te and can be ignored during electrowinning. Se and Te show similar thermodynamic behaviour in aqueous solution but Se was not deposited due to its low electrical conductivity and low concentration.

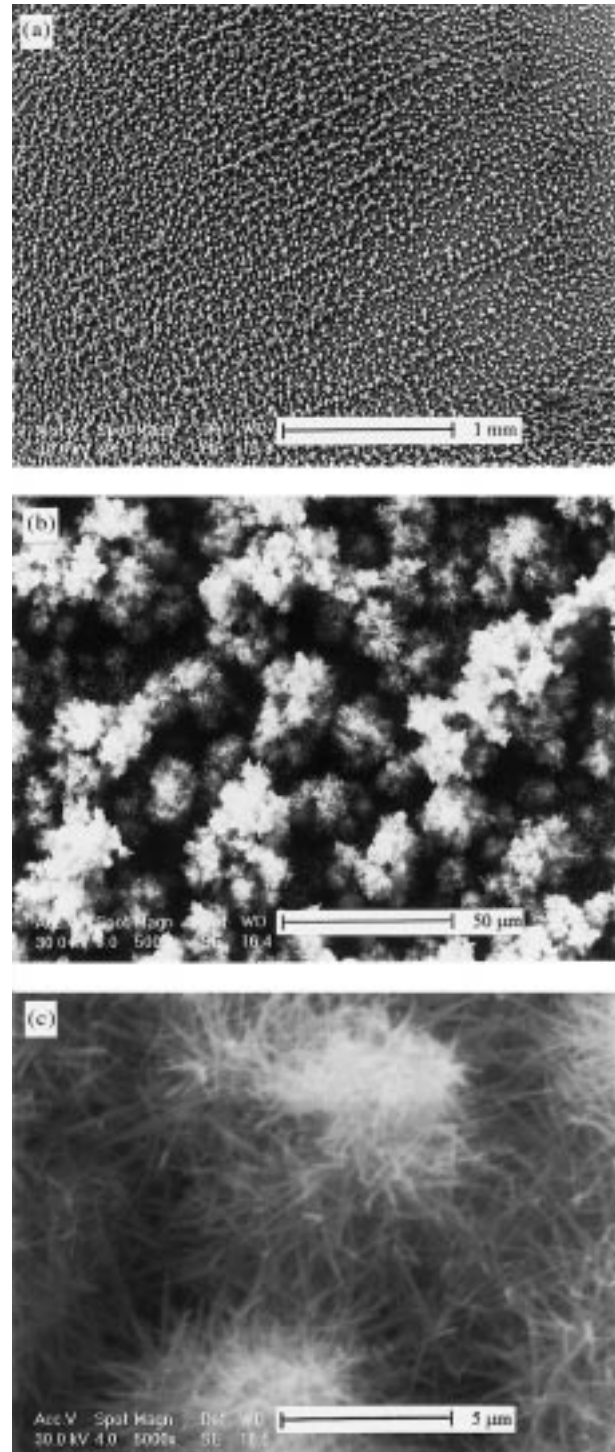


Fig. 11. Morphology of the tellurium deposit on an SS plate obtained by the potentiostatic experiment with applied potential of -0.8 V .

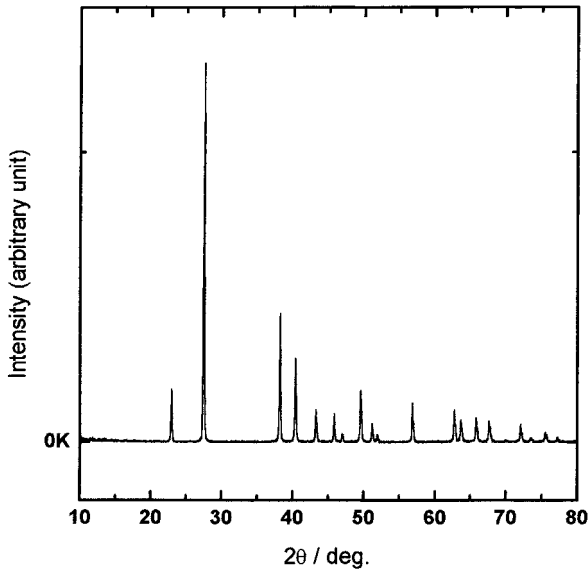


Fig. 12. Powder diffraction pattern of electrodeposited Te with applied potential of -0.8 V.

3.2.2. Laboratory-scale electrowinning

A laboratory-scale electrolytic cell with a cathode area of 7.5 cm² and an interelectrode distance of 6.5 cm was used to recover Te from alkaline leach liquor of cemented Te. The recovery rate and current efficiency were studied under different conditions such as applied voltage, temperature and initial Te concentration.

Figure 13 illustrates the effect of applied voltage on the electrowinning of Te. The time necessary to recover the Te was shortened with increase in applied voltage. However, higher voltage caused severe hydrogen evolution and the current efficiency dropped rapidly. Thus a voltage of 4 V can be specified as optimum.

Figure 14 shows the effects of temperature on the electrowinning of Te at a voltage of 4 V. At elevated

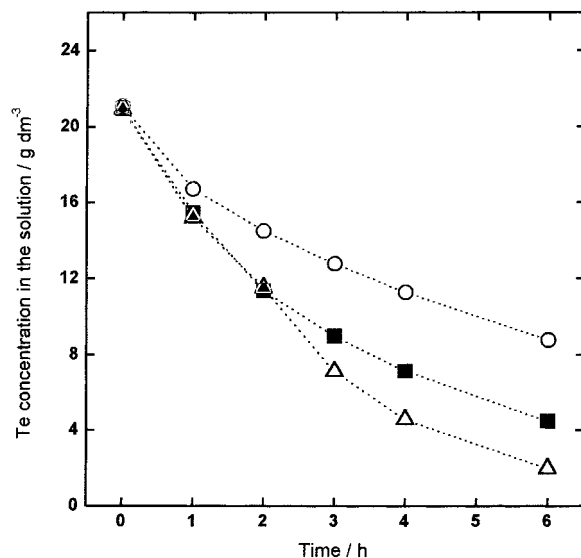


Fig. 13. Variation of Te concentration during the potentiostatic electrowinning with different applied voltages (initial Te concentration: 21 g dm⁻³, ambient temperature). Key: (○) 3, (■) 4 and (△) 5 V.

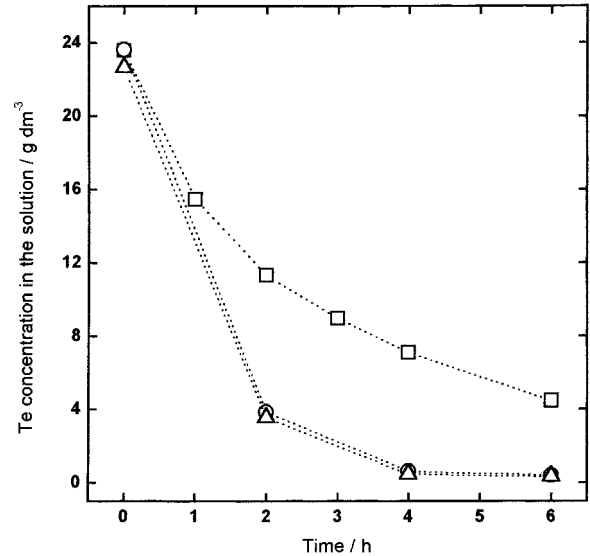


Fig. 14. Variation of Te concentration during the potentiostatic electrowinning with at different temperatures (applied voltage 4 V; initial Te concentration 21 g dm⁻³). Key: (□) room temp., (○) 40 °C and (△) 60 °C.

temperature, tellurium was recovered more rapidly but hydrogen evolution occurred more vigorously and decreased the current efficiency. As a result, a temperature of about 40 °C can be recommended for a faster recovery and lower energy consumption.

From the current profile of the potentiostatic experiment shown in Figure 10, where the initial current transient behaviour exists for about an hour, galvanostatic electrowinning can be recommended for faster recovery. Under the galvanostatic condition with an applied current density of 25 mA cm⁻², the effect of the initial Te concentration was investigated and is shown in Figure 15, where the operating temperature was 40 °C.

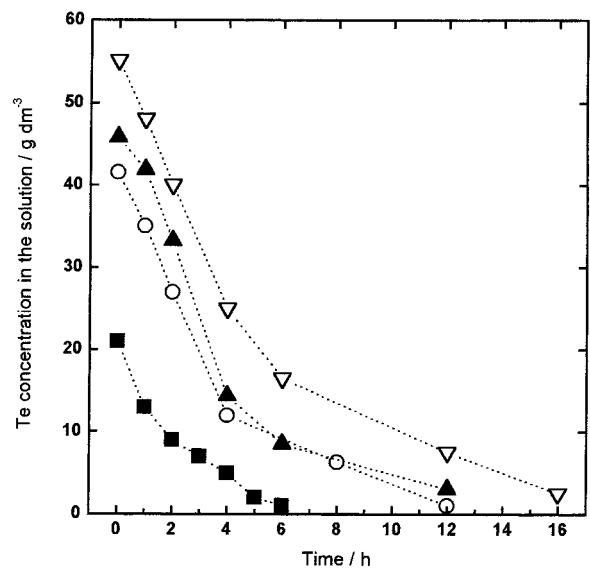


Fig. 15. Variation of Te concentration during the galvanostatic electrowinning. Different initial Te concentrations (applied current density 25 mA cm⁻², 40 °C): (■) 21.0 , (○) 41.5 , (▲) 45.8 and (▽) 55.1 g dm⁻³.

Table 1. Recoveries and current efficiencies of electrowinning of Te under various galvanostatic conditions

Initial Te concentration /g dm ⁻³	Recovery /%	Current efficiency /%
55.1	56.1	87.9
55.1	85.4	55.0
45.8	45.4	97.1
45.8	93.4	50.5
41.5	34.9	98.0
41.5	88.0	61.3
21.0	57.1	84.0
21.0	90.5	53.2

(Applied current density: 25 mA cm⁻², 40 °C)

Table 2. Chemical composition of electrodeposited Te metal (in ppm)

Element	Cu	Se	As	Sb	Pb	Fe	Zn	Bi
Content	10	240	40	5	42	36	28	5

The recovery rate increases with increasing initial Te concentration, which is determined and limited by the leaching process.

Table 1 shows the current efficiencies under various galvanostatic experiments. They were about 85–95% for 50% recovery and about 50–60% for 90% recovery. Considering the recovery rate as well as the current efficiency, 50% recovery of Te followed by circulating the spent electrolyte after mixing with fresh leach liquor is recommended. The purity of the Te electrowon was higher than 99.95% and major impurities are shown in Table 2.

4. Summary

To study the feasibility of the electrowinning process for the recovery of tellurium from alkaline leach liquor of cemented Te, the electrochemical behaviour of tellurium and its deposition characteristics were analysed by electrochemical techniques, SEM and XRD techniques. Tellurite ion showed stepwise reduction to tellurium and to ditelluride ion in alkaline solution and the potential range for a stable tellurium deposit on metals such as Pt and SS was within 150 mV. The ditelluride ion can

disproportionate to tellurium and telluride ion and the latter can react with tellurite ion to produce a precipitation of colloidal Te; more negative potentials below –0.95 V can be applied for electrowinning process. The deposit of tellurium showed very porous morphology with needlelike radial growth in the pores. With Na₂S purification processes, highly pure Te metal was recovered by electrowinning and the purity of tellurium was higher than 99.95%. The current efficiency for the electrowinning process was affected by the applied voltage, the initial Te concentration and temperature. As the applied voltage increased, the current efficiency fell due to the hydrogen evolution reaction. Higher initial Te concentration and lower temperature showed higher current efficiency, but a longer time was necessary for the recovery of Te. The optimum operation for the electrowinning of Te under galvanostatic conditions was identified as 50% recovery of tellurium followed by circulating the spent electrolyte after mixing with fresh leach liquor at a temperature of about 40 °C.

References

1. E. Hoffmann, *JOM* **41**(7) (1989) 32.
2. K.-I. Rhee, C.-K. Lee, C.-S. Yoo, T.-H. Kim, H.-S. Kim and H.-J. Sohn, Proceedings of the EPD Congress 1997, TMS, Orlando, FA, 9–13 Feb. (1997), p. 495.
3. J.J. Lingane and L.W. Niedrach, *J. Am. Chem. Soc.* **70** (1948) 4115.
4. J.J. Lingane and L.W. Niedrach, *J. Am. Chem. Soc.* **71** (1949) 196.
5. A.J. Panson, *J. Phys. Chem.* **67** (1963) 2177.
6. R.A. Jemieson and S.P. Perone, *J. Electroanal. Chem.* **23** (1969) 411.
7. K.K. Mishra, D. Ham and K. Rajeshwar, *J. Electrochem. Soc.* **137** (1990) 3483.
8. M. Pourbaix, 'Atlas of Electrochemical Equilibria in Aqueous Solution', 2nd edn., NACE, Houston TX (1974), p. 560.
9. G. Trejo, A.F. Gil and I. González, *J. Appl. Electrochem.* **26** (1996) 1287.
10. Y. Castrillejo, A.M. Martinez, M. Vega and P.S. Batanero, *J. Appl. Electrochem.* **26** (1996) 1279.
11. E. Gómez, J. Ramirez and E. Vallés, *J. Appl. Electrochem.* **28** (1998) 71.
12. S.I. Zhdanov, 'Encyclopedia of Electrochemistry of the Elements', Vol. 4 (Marcel Dekker, New York, 1974), p. 393.
13. B. Handle, G. Broderick and P. Paschen, *Hydrometallurgy* **46** (1997) 105.
14. J. Jorné and M.C. Lee, *J. Electrochem. Soc.* **143** (1996) 865.